WEC 8-5112-MPR-15
cy. 2

N64-18444
CODE-1
CR-53579

1 Mp.

OTS PRICE
XEROX $ 1.60 ph
MICROFILM $ 0.80 mf.

Westinghouse

ELECTRIC CORPORATION

Monthly Progress Report No. 15

Development Of An Image Converter

of Radical Design

(Phase II)

~~Period~~ 1 September ~~to~~ 30 September 1963

(NASA Contract NAS 8-5112)

0 pers auth. 3 October 1963 17p ref.

2446292 **WESTINGHOUSE ELECTRIC CORPORATION**

Air Arm Division

Baltimore, Maryland

12 OTS

(NASA CR-53579)

OTS: $1.60ph, $0.80mf

ABSTRACT

A

Examination of "enlarged area" image converter matrices has continued to determine device characteristics and to pinpoint fabrication problem areas.

Design of a preliminary peripheral readout system for a 5 x 5 matrix system is in progress and laboratory testing of readout circuits will be initiated shortly.

System studies to establish technical requirements for both the image converter and peripheral equipment are continuing.

TABLE OF CONTENTS

LIST OF ILLUSTRATIONS

1.0 INTRODUCTION AND SUMMARY

The objective of this program is the development and fabrication of a 50 x 50 element photo transistor mosaic and design of peripheral equipment to permit readout of the mosaic output signals.

Phototransistor matrices produced to date had at times been characterized by poor collector isolation, and low sensitivity, as well as poor uniformity and difficult reproducibility. Major program effort is being devoted to finding solutions to these problems and some progress has been achieved.

A system study has been carried out to establish a sensitivity equation for matrix type imaging systems. These studies are continuing to establish specifications for both the photo-transistor matrix and the overall system.

Laboratory measurements indicate that the average sensitivity of current mosaic elements is about 1/4 to 1/10 that of typical single element photo transistors.

Peripheral equipment studies are continuing using the data obtained from the laboratory measurements to establish tentative mosaic specifications. At this time it appears that a significant portion of the peripheral equipment can be molecularized with little cost penalty.

2.0 INVESTIGATIONS AND RESULTS DURING THE CURRENT REPORTING PERIOD

2.1 Image Converter Development

Efforts have continued to establish the causes and cures of difficulties experienced to date in the photo-sensor mosaic development program. In addition, efforts have been intensified to establish a more optimum sensor structure.

2.1.1 EVALUATION OF CURRENT MOSAIC FABRICATION ACTIVITY

Units produced during September continued to exhibit characteristics similar to those of previous mosaics. More extensive in-process testing has permitted earlier detection of deficient devices, thereby focusing attention on more specific problems. Adequate isolation (as furnished by the diffused isolation regions) remains a serious problem, although it has considerably improved over earlier units. While efforts are continuing to solve this problem directly, some attention is being directed toward use of a simpler structure, as described in paragraph 2.1.3.

2.1.2 COLLECTOR JUNCTION DEPTH OPTIMIZATION

An optimum depth exists for the base-collector junction of a silicon phototransistor for a given wave length distribution of incident radiation. This depth is such that a maximum number of photons will be absorbed in a region of the base sufficiently near to the collector junction so that electrons (of the photon-created hole-electron pairs) will diffuse to the depletion region about the collector junction. The holes, because of their lower mobility as well as the retarding fields at the junctions, remain trapped in the base and act to bias the emitter-base junction in the forward direction. This accounts for the phototransistor current gain. The measured photocurrent is approximately equal to the photon generated current (plus the dark current) flowing across the collector-base junction multiplied by the gain of the transistor.

In a previous series of experiments attempts were made to fabricate phototransistors with emitter, base, and collector resistivities the same in each device but with varying depths of the base-collector junction. In order to maintain identical base widths the locations of the emitter-base junctions had to be varied. This series of experiments did not yield a great deal of useful information primarily because of poor junction characteristics, largely due to the fabrication complexity necessary to keep resistivity and base width parameters constant while varying junction depths.

As stated above, $I_{CEO} \sim \beta I_{CBO}$. The question of optimizing collector junction depth in the transistor may be approximated by investigating the photoresponse of collector-base pn junction diodes. Although these may have various junction depths the P and N regions will be of the same resistivity as the respective P and N regions of the transistor base and collector. A program of this nature has been initiated, and models should be fabricated in October.

2.1.3 SIMPLIFIED MOSAIC GEOMETRY

Considerable thought has been devoted to the desirability and feasibility of simplifying both the device geometry and fabrication processes. As a first step, a strip collector design was considered as reported in the last monthly report. The advantage of this design would be the elimination of a significant portion of the isolation junction perimeters as well as elimination of significant portions of the deposited aluminum interconnection patterns from the surface of the mosaic. Tests performed with the base contacts provided on the new photo-transistor mosaics indicate that a common collector configuration might be feasible. In such a mosaic, XY readout would be accomplished through the use of the base and emitter leads. This would eliminate the isolation junctions completely and would significantly simplify mosaic fabrication. The feasibility of this concept will be explored using a photo-transistor mosaic of individual elements during the next period. If these tests are successful, design of fabrication masks for a mosaic will be produced. Until these tests are completed, development of the strip collector masks has been tabled.

2.2 Image Converter Packaging

Effort has continued on various aspects of the package for the 50 x 50 image converter mosaic. An artist's conception of this package was given in the previous report. During this period effort was devoted primarily to methods of connecting the pads at the end of the metallized strips (which connect elements in a line) to the leads of the package. A mask to provide this function by vacuum evaporated aluminum interconnections is in preparation.

2.3 Peripheral Equipment and System Analysis

2.3.1 SYSTEM STUDIES

System studies which developed a general equation for system sensitivity were reported in the last report. Appendix I presents the results of these studies for this period, relating the general equation from the last report to a mosaic imaging system in terms of field of view, frame rate, system optics, and conversion efficiencies.

These studies will be continued to establish a tentative system specification in the next period, based on the results of optical bench evaluation of typical photo transistor devices.

2.3.2 5 x 5 MOSAIC PERFORMANCE

Measured optical-electrical performance data was obtained on an enlarged 5 x 5 mosaic. To obtain steady-state data the optical bench was used with a filament type light source at a color temperature of 2400°K. A spot of light .031" diameter (matched to the detector element size) was used to measure the response of a randomly chosen 5 of the 25 elements in a matrix array. The response characteristics are shown in Table I and in Figures 1, 2 and 3. A relatively important lack of uniformity at low input levels characterized this particular mosaic. This is possibly due to surface leakage characteristics and indicates the severe nature of surface problems. It is felt that this condition can be alleviated in future devices. However, an appropriate readout scheme can be utilized in conjunction with such a device to obtain useful image conversion data.

The mosaic is normally operated with the collector junction reverse biased. Bias levels of greater than 25 Volts could be used since this was below junction breakdown. At reasonable bias levels the slope of the signal (or dark current) versus collector voltage curves were desirably small. This means that small variations in the collector voltage will not appear at the sensor output as a spurious signal. The element is normally operated with the base lead open and the emitter grounded. Small values of positive base bias increase the flow of collector (or dark) current. If the positive base bias is large it effectively masks the normal signal current. Negative base bias reduces element light sensitivity and dark current. Separate biasing of each element to equalize sensitivity uniformity, reduce leakage current, and improve linearity is a possibility but its cost is that of cross connection complexities and critical bias adjustments.

The mosaic tested was an enlarged structure whose sensitive elements were 16 times larger in area than the elements in the normal 5 x 5 and 50 x 50 mosiacs. The data in Table I is the average data from 3 elements of the mosaic which had median characteristics in uniformity and sensitivity (Figure 1). In spite of the transistor electrical gain of approximately 20, the computed quantum efficiency is only 9.2 percent. This is probably because the exposed area of the sensitive base is limited to less than 15% of the available element area, the remainder being taken up by isolation junction, collector junction, emitter, and interconnections. Also some photon absorption occurs in the silicon, and carriers which are created near the surface may not have sufficient lifetime to diffuse to the active area around the collector junction.

The Noise Equivalent Power, NEP, is computed relative to element dark current rather than r.m.s. noise. This was because the noise bandwidth of the low level DC amplifier was about 10 cps. For a 5 x 5 matrix swept at TV field rates, the noise bandwidth of the amplifier will be only 1500 cps. For a 50 x 50 matrix the noise bandwidth will be 150 Kc.

The dynamic range of the device appears to be considerable. The upper light level limit may be determined more by incident thermal effects than by internally generated heat due to large currents (at least for units of only moderate current gain). Based on the measurements, the photocurrent has not saturated at incident light levels of 20,000 foot lamberts.

2.3.3 PERIPHERAL READOUT EQUIPMENT

With the measured characteristics of preliminary mosaic characteristics being obtained, it now becomes possible to determine properties of the readout equipment necessary to provide useful image conversion data.

If the mosaic is to be sensitive to light levels of the order of 1 FL, photocurrents of the order of tens of nanoamps provide the useful signal output. This low level imposes severe low noise requirements on the preamplifier and severe cutoff current and offset voltage requirements on the matrix readout switches. Photoconductive switching provides very low

Table I

5 x 5 Matrix Array (Enlarged Structure)
Average Steady State Characteristics for 5 Randomly Chosen Elements
Ambient Temperature 25°C

Gross Size of Element	.04" x 04" = .0016 sq. in.
Sensitive Size of Element	.000236 sq. in.
Illuminance Spot Size	.031" Dia = .00078 sq. in.
Resolution - No. Elements (or lines) per inch	25
Dark Current	.01 ua at 25V (See Fig. 1)
Light Responsivity	.01 ua/FL at 25V and 2 FC (Fig. 1)
Sensitivity Uniformity	15:1 at 2 FC (See Fig. 2)
Linearity	Compression occurs at upper Light levels (See Fig. 1). The linearity is better and extends over a greater range for electron injected carriers than for photon injected carriers.
Isolation	1. Optical: (one element illuminated, nearby element read out). Good. 2. Electrical: (current in one element due to bias on neighboring element (dark)). Poor. 3. Masking is required to prevent light from injecting carriers into the isolation junctions.
Transistor Gain (β)	20
Conversion Efficiency	9.2%
Detectivity, NEP_{DC}	7.8×10^{-6} watts
Collector Breakdown BV_{CEO}	greater than 25V
Illumination Range	2 Foot Lamberts to 20,000 FL
Output Range	Approximately .02 ua to 60 ua

noise operation for small-signal switching, tends to minimize switching transients and any tendency to ring and provides convenient isolating coupling between the pulse generator and the switch. The photoconductor transistor rise and fall time is in the range of 1 to 10 microseconds which is adequate for a 5 x 5 matrix readout. If neon lamp control elements are used, a rather large breakdown voltage is required to drive the neon. The spectral characteristics of neon are within the most sensitive response regions of silicon, but the light flux output is a minimum in order to drive a phototransistor. If the neon source is driven harder, more power is consumed with a consequent blackening of the interior of the neon bulb and reduced constancy of output and lifetime. Electrostatic shielding may be necessary between the neon and the switch.

As seen from Figure 2 and Figure 3 the nonuniformity of the elements is large in this first available batch of enlarged 5 x 5 element matrices. It is anticipated that better batch uniformity will result as more experience is gained in the construction of these devices. In an experimental production lot of transistors that have been produced for about a year in this laboratory, noise figure and gain distributions normalize about an acceptable median as shown in Figure 4. When this occurs for the mosaic, signal processing procedures will be devised as part of the peripheral equipment to equalize different gain increments and dark currents in the elements of the sensor.

Element leakage characteristics and element generated noise are other factors that have to be considered in signal processing schemes. As stated before a large part of the element leakage is due to surface problems and it is anticipated that this condition can be alleviated in future devices. For a 5 x 5 element mosaic swept at a TV frame rate of 60 cps, the noise equivalent bandwidth of the system will be only 1500 cps. This is good. However, in photoresponsive devices, it appears 1/f noise extends up to a frequency of 10 Kc and therefore will also limit the minimum light level which can be detected by the device. On the contrary, operation at low light levels permits the elements in the mosaic to be operated under "starved" conditions and therefore noise should be minimized.

3.0 PROGRAM FOR THE ENSUING PERIOD

3.1 Image Converter Model Development

The present structure of enlarged 5 x 5 image converter transistor mosaics will be utilized for further fabrication and analysis. Fabrication evaluation and control procedures will be enhanced by incorporating additional microscopic inspection, electrical testing, and metallurgical analysis steps to those already extant in the process. By the conclusion of the ensuing reporting period the study of collector junction depths, described above in paragraph 3.1, should have reached the point at which the elements to be studied will have been fabricated and their response to visible radiation will be under examination.

3.2 Image Converter Packaging

It is anticipated that a completed package for the 50 x 50 photosensor array will be available during the next period. The external package leads will be of the flexible soldered type. Effort will be focussed on a masking procedure which will result in an evaporated metal conducting strip over the insulating glass is complete the connection from device to package terminals.

3.3 Peripheral Equipment

As more mosaics become available further sensitivity and linearity tests will be made.

Molecular logic devices for the readout equipment will be obtained and construction of the pulse and switching circuitry will be initiated.

Appendix I

The General Equation for System Sensitivity
Specific System Sensitivity Expression
(Continued from Monthly Progress Report 14)

Mosaic Sensor

The mosaic sensor is essentially an array of point detectors covering the entire field of view of the system. The sensor geometry is shown in Figure 5.

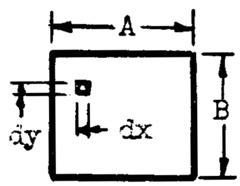

Figure 5
Mosaic Sensor Geometry

A = Total Azimuth Field of View to be surveyed (degrees
B = Total Elevation Field of View to be surveyed (degrees)
T_f = Frame time required for surveillance of total field of view (sec)
fr = $1/T_f$ frame rate
m = Number of elements in X direction
n = Number of elements in Y direction

To optimize the peak signal to rms noise ratio the system's signal processing bandwidth Δf is set equal to the reciprocal of the dwell time T_D of the instantaneous field of view:

$$\Delta f = \frac{1}{T_d} \ (\text{sec}^{-1}) \qquad (11)$$

The dwell time, T_D, is equal to the frame time T_f divided by the total number of discrete elements m times n in the mosaic

$$T_d = \frac{T_f}{mn} \ (\text{sec}) \qquad (12)$$

Therefore

$$\Delta f = \frac{mn}{T_f} = m \ n \ f_r \ (\text{sec}^{-1}) \qquad (13)$$

Substituting equation (13) into equation (10) of Monthly Progress Report 14 yields the mosaic sensitivity equation:

$$\theta = \frac{4F\ (m\ n\ dx\ dy\ f_r)^{\frac{1}{2}}}{\pi\,(57.3)\ C_s T_o D_o D^*}\ \text{watts/cm}^2 \qquad (14)$$

Since the mosaic array consists of m times n elements each having an instantaneous field of view of dx times dy the total field of view AB:

$$A \times B = (m\ dx)\ (n\ dy)\ (\text{degrees}^2) \qquad (15)$$

The sensitivity equation may now be written:

$$\theta = \frac{4F\ (ABfr)^{\frac{1}{2}}}{\pi\,(57.3)\ C_s T_o D_o D^*}\ \text{watts/cm}^2 \qquad (16)$$

Equation (14) and (16) describe the system sensitivity of a mosaic detector of an imaging system in terms of the optical parameters, the number of detector elements and the detector Figure of Merit. The equations show that sensitivity is enhanced by a high quality, fast optical system and by high detector figure of merit D*. A large field of view degrades sensitivity. As frame time increases sensitivity is improved.

These equations were derived for an optical system whose performance is limited by noise in the detector unit. Other system performance limitation factors such as dark current, leakage, and non-uniform gain and sensitivity characteristics of the detector and switching noise from the readout equipment would have to be accounted for in another manner.

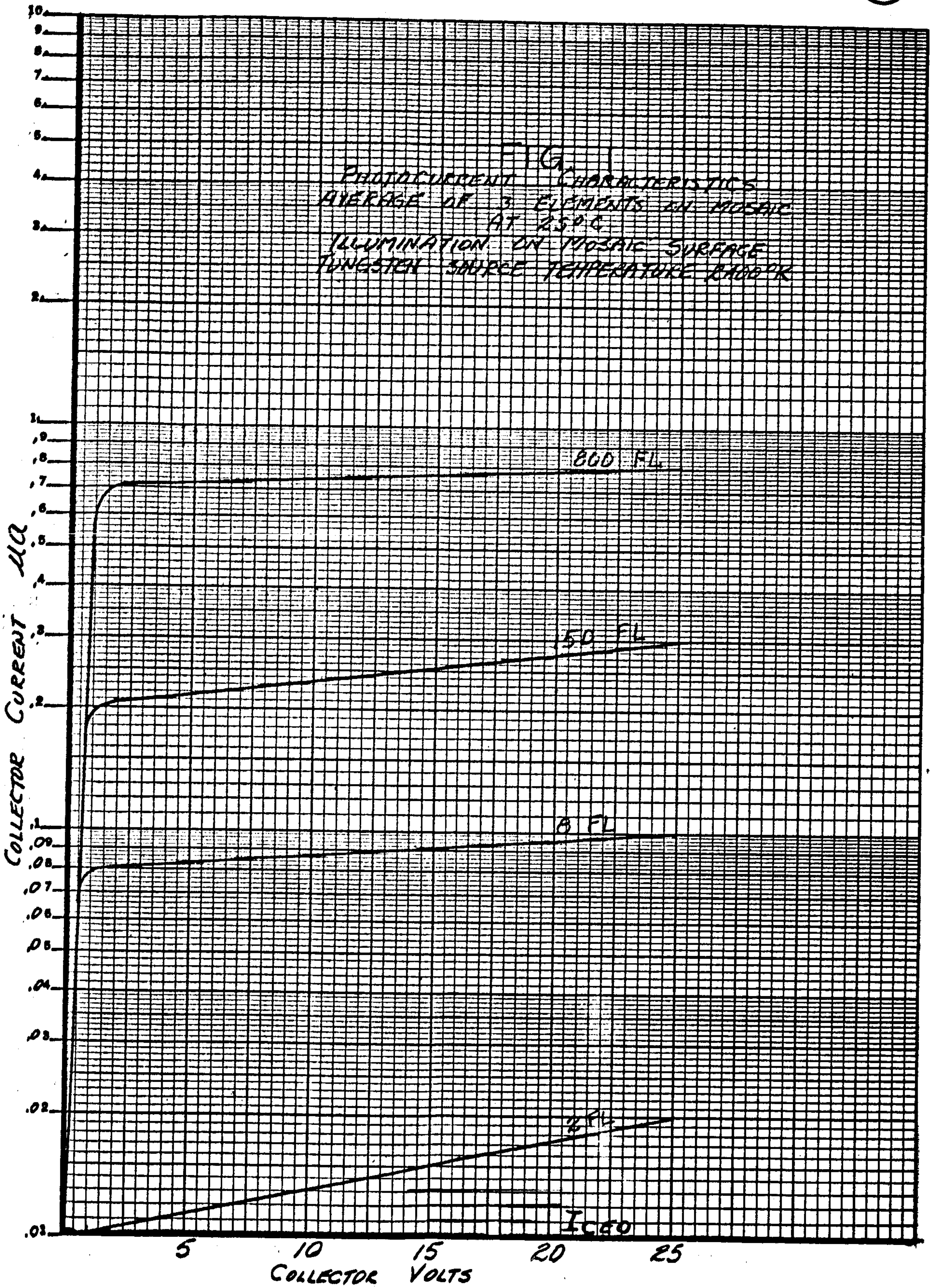
FIG.
PHOTOCURRENT CHARACTERISTICS
AVERAGE OF 3 ELEMENTS IN MOSAIC
AT 25°C
ILLUMINATION ON MOSAIC SURFACE
TUNGSTEN SOURCE TEMPERATURE 2800°K
800 FL
150 FL
8 FL
2 FL
ICEO
COLLECTOR CURRENT μa
COLLECTOR VOLTS
5
10
15
20
25
10
9
8
7
6
5
4
3
2
1
.9
.8
.7
.6
.5
.4
.3
.2
.1
.09
.08
.07
.06
.05
.04
.03
.02
.01

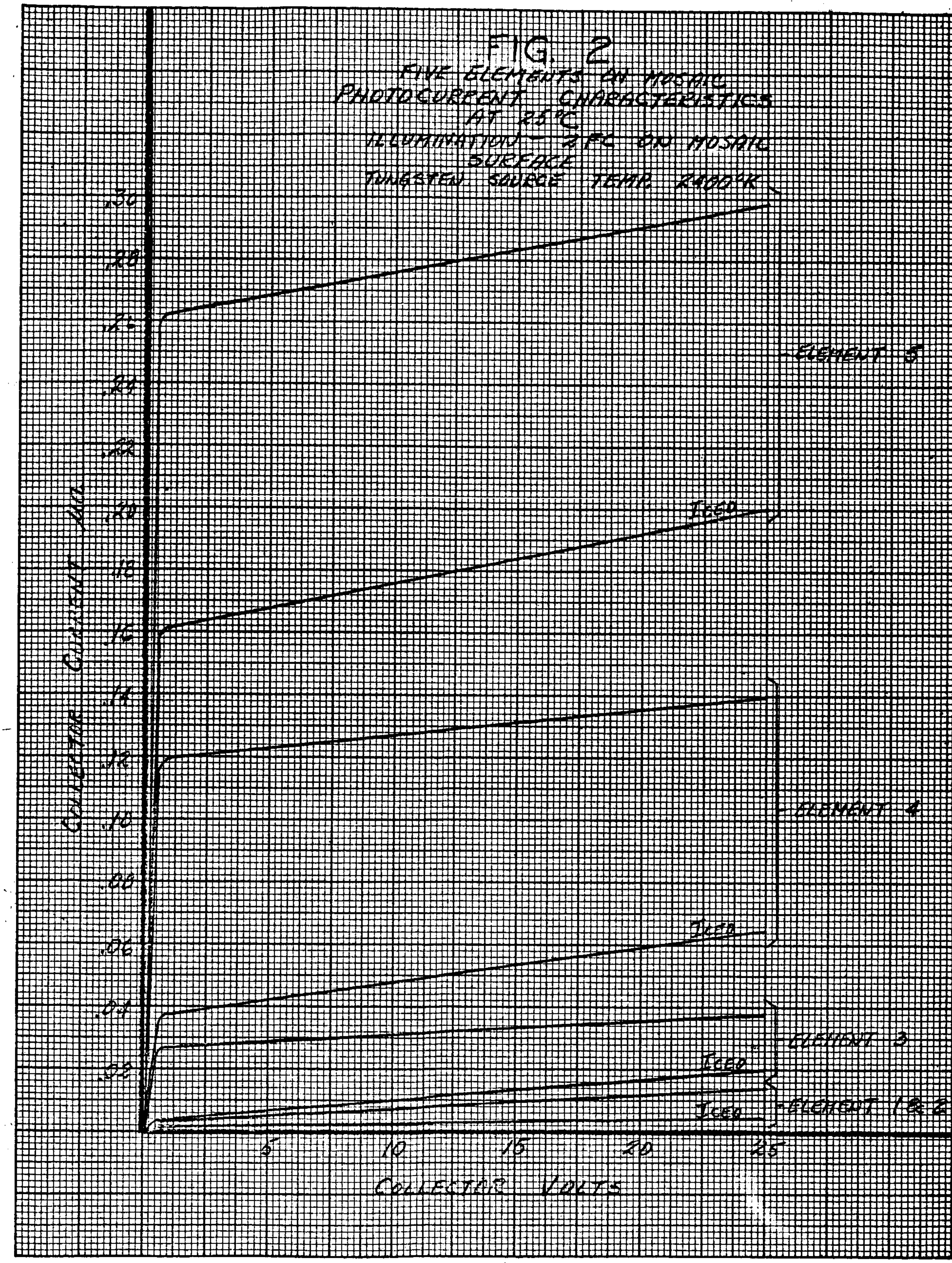
FIG. 2
FIVE ELEMENTS IN MOSAIC
PHOTOCURRENT CHARACTERISTICS
AT 25°C
ILLUMINATION - 2FC ON MOSAIC
SURFACE
TUNGSTEN SOURCE TEMP. 2400°K
COLLECTOR CURRENT MA.
.30
.28
.26
.24
.22
.20
.18
.16
.14
.12
.10
.08
.06
.04
.02
ELEMENT 5
ICEO
ELEMENT 4
ICEO
ELEMENT 3
ICEO
ELEMENT 1 & 2
ICEO
5
10
15
20
25
COLLECTOR VOLTS

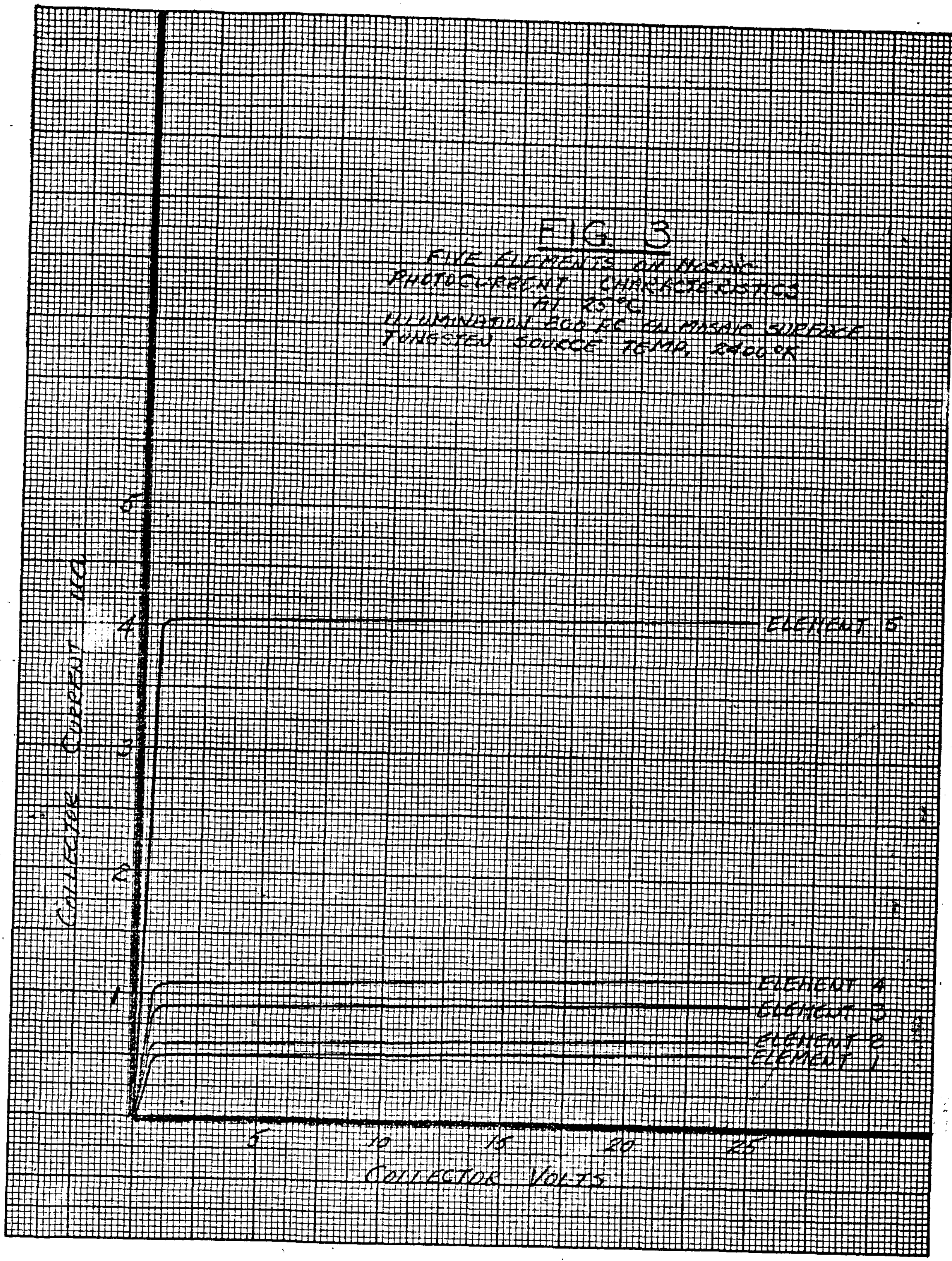
FIG. 3
FIVE ELEMENTS ON MOSAIC
PHOTOCURRENT CHARACTERISTICS
AT 25°C
ILLUMINATION 200 FC ON MOSAIC SURFACE
TUNGSTEN SOURCE 75MA, 2400°K
COLLECTOR CURRENT μa
1
2
3
4
5
ELEMENT 5
ELEMENT 4
ELEMENT 3
ELEMENT 2
ELEMENT 1
5
10
15
20
25
COLLECTOR VOLTS

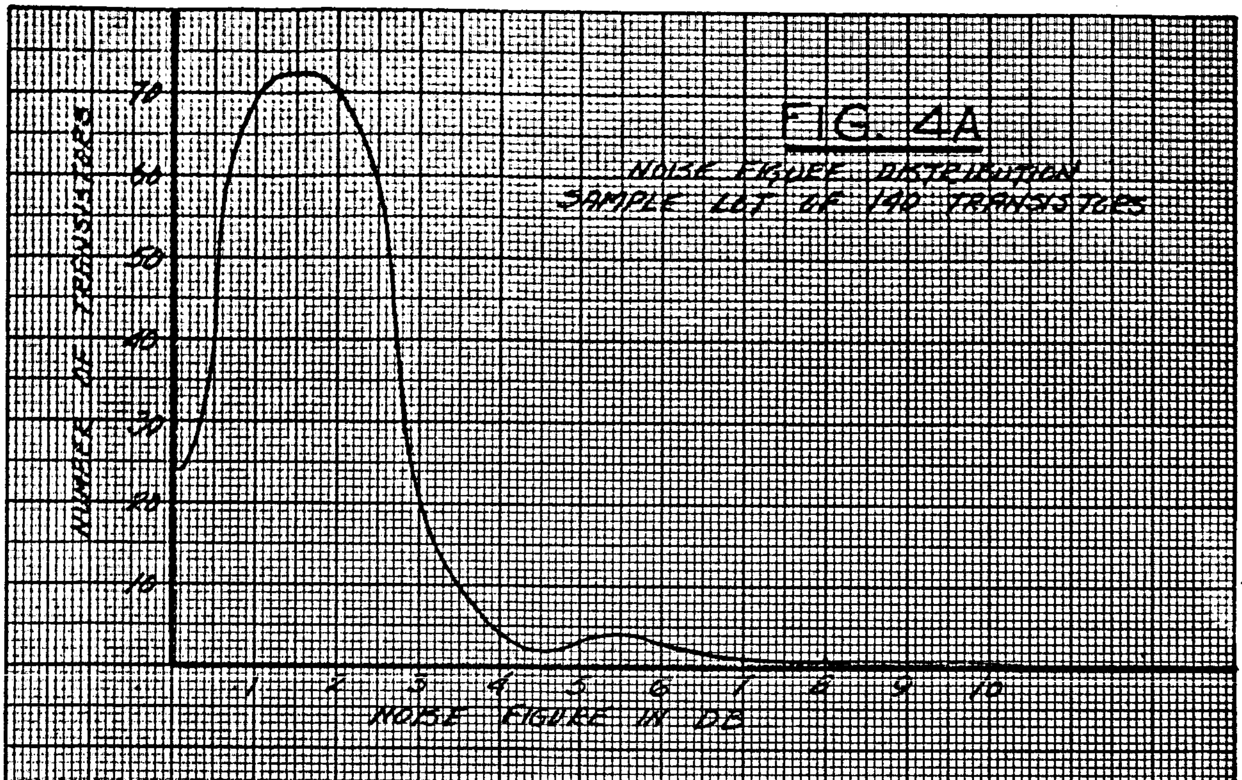
FIG. 4A
NOISE FIGURE DISTRIBUTION
SAMPLE LOT OF 190 TRANSISTORS
NUMBER OF TRANSISTORS
70
60
50
40
30
20
10
1
2
3
4
5
6
7
8
9
10
NOISE FIGURE IN DB

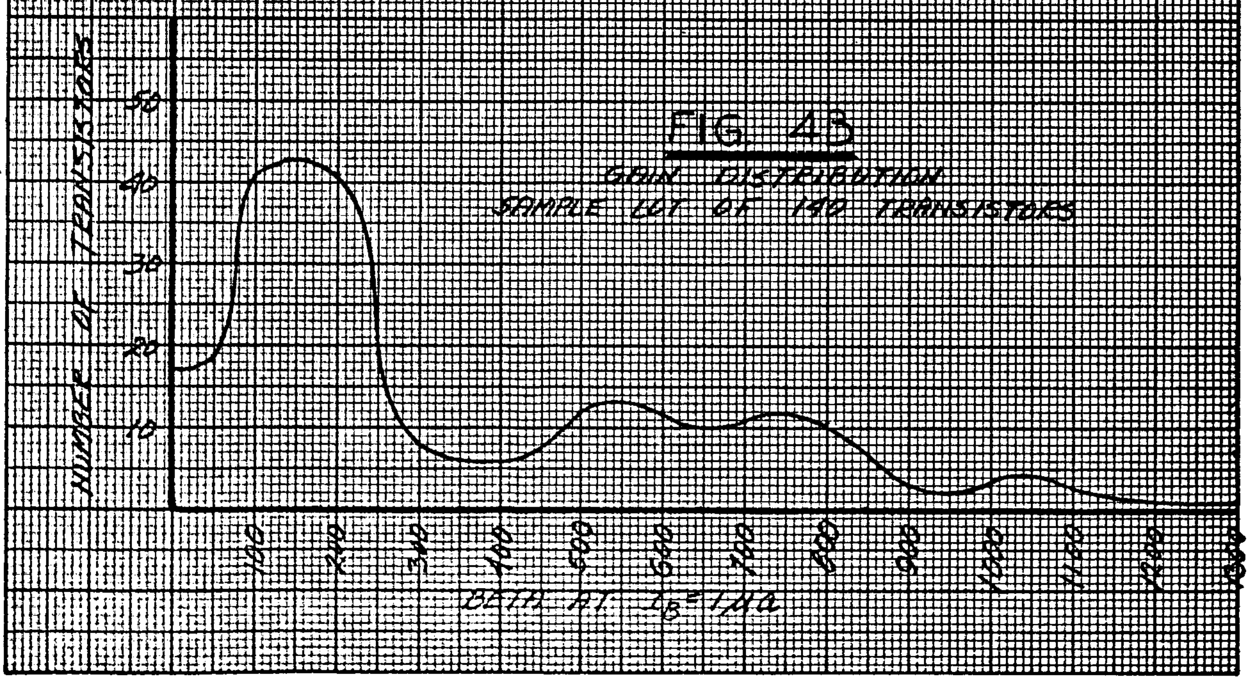
FIG. 4B
GAIN DISTRIBUTION
SAMPLE LOT OF 190 TRANSISTORS
NUMBER OF TRANSISTORS
50
40
30
20
10
100
200
300
400
500
600
700
800
900
1000
1100
1200
1300
BETA AT IB = 1 MA